



# Use of machine learning algorithms for surface roughness prediction of printed parts in polyvinyl butyral via fused deposition modeling

Azahara Cerro<sup>1</sup> · Pablo E. Romero<sup>1</sup> · Okan Yiğit<sup>2</sup> · Andres Bustillo<sup>3</sup>

Received: 7 January 2021 / Accepted: 17 May 2021 / Published online: 25 May 2021

© The Author(s), under exclusive licence to Springer-Verlag London Ltd., part of Springer Nature 2021

## Abstract

Machine learning algorithms for classification are employed in this study to generate different models that can predict the surface roughness of parts manufactured from polyvinyl butyral by means of Fused Deposition Modeling (FDM). Five input variables are defined (layer height, print speed, number of perimeters, wall angle, and extruder temperature), and 16 parts are 3D printed, each with three different surfaces (48 surfaces in total). The print values used to print each part were defined by a fractionated orthogonal experimental design. Using a perthometer, the average value of surface roughness,  $Ra$ , on each surface was obtained. From these experimental values, 40 models were trained and validated. The model with the best prediction results was the one generated by bagging and Multilayer Perceptron (BMLP), with a Kappa statistic of 0.9143. The input variables with the highest influence on the surface finish are the wall angle and the layer height.

**Keywords** Machine learning · 3d printing · Fused deposition modeling · Fused filament fabrication · Surface roughness · WEKA

## 1 Introduction

Additive manufacturing technologies (AM) are increasingly used in industry for two central reasons: on the one hand, these disruptive technologies have a large number of advantages over conventional manufacturing technologies; on the other hand, many of the weaknesses associated with AM, such as the variable quality of manufactured parts, can be addressed with the help of machine learning [1–3].

Fused Deposition Modeling (FDM) is one of the most widespread additive manufacturing technologies [4] for the following reasons: low cost, high speed, and the simplicity of the process. The FDM process consists of melting and extruding a continuous filament of thermoplastic polymer. The melted filament is deposited layer by layer until it forms the desired part. The materials used most frequently in FDM are [5, 6]: ABS, PLA, PETG, PC, and ULTEM.

Dozens of parameters are involved in the printing of a part via FDM. It is difficult to know which values are the most suitable for printing a part with one specific characteristic or another [7, 8]. Over recent years, machine learning techniques have been used in FDM printing processes, with different objectives: to improve viscoelastic responses [9]; to predict maximal printable bridge length and to minimize support waste [10]; to forecast the dynamic moduli of elasticity for load-carrying parts under cyclic conditions [11]; to predict tensile strength corresponding to different raster patterns [12]; to increase wear resistance [13]; and to enhance compressive strength [14].

Ensuring adequate surface integrity is a major problem for FDM printed parts [15]. Some authors have tried to predict the surface roughness of FDM printed parts based on printing parameters, using models generated by machine learning. Boschetto *et al.* [16] used feed-forward neural networks to predict surface roughness in parts printed on ABS, ABS plus,

✉ Pablo E. Romero  
p62rocap@uco.es

Azahara Cerro  
azaharacerro@gmail.com

Okan Yiğit  
okan.yigit@outlook.com.tr

Andres Bustillo  
abustillo@ubu.es

<sup>1</sup> Department of Mechanical Engineering, University of Cordoba, Medina Azahara, 5, 14071 Cordoba, Spain

<sup>2</sup> Department of Mechanical Engineering, University of Karabuk, Kastamonu Yolu Demir Celik Kampusu, 78050 Karabuk, Turkey

<sup>3</sup> Departamento de Ingenieria Informatica, University of Burgos, Avda Cantabria s/n, 09006 Burgos, Spain

Polycarbonate and ULTEM 9085. Vahabli and Rahmati [17] sought to predict the surface finish on 3D printed parts by means of FDM, using multilayer perceptron neural networks. The main novelty they introduced was the use of different learning functions: Levenberg-Marquardt (LM), Particle Swarm Optimization (PSO), and Imperialist Competitive Algorithm (ICA). The printing material they used was ABSplus. These previous works share certain characteristics: they use common materials, such as ABS or PC; they use neural networks to predict the surface roughness obtained (solving regression problems); their models only consider two variables: height of layer and angle of inclination.

Prediction of the exact surface roughness value of a part (regression problem) can be of interest for certain purposes. However, in other cases, it may be sufficient to know whether the surface finish to be obtained is medium or rough (classification problem) [3]. In fact, the standards used until a few years ago in industry used classes when defining surface roughness [18]; for example, N11 is the class that corresponds to a surface roughness between 12.5 and 25  $\mu\text{m}$ ; N12 is the class that corresponds to a surface roughness between 25 and 50  $\mu\text{m}$ . It may therefore be of interest to generate models for predicting whether the roughness class is N11 or N12. Studies can be found in the literature that use these sorts of classification algorithms, to determine the surface finish (good or bad) of parts manufactured by other printing technologies [19].

In the present work, the use of machine learning algorithms is proposed to predict the surface finish of 3D FDM printed parts. In this study, the specimens were printed on polyvinyl butyral, a material that has hardly been studied and that, in addition to showing reasonable mechanical behavior, will when polished with alcohol become transparent [20]. The problem to be solved is not a regression problem, but a classification problem: it is a question of predicting, depending on the input variables, whether the surface roughness will be class N11 (between 12.5 and 25  $\mu\text{m}$ ) or N12 (between 25 and 50  $\mu\text{m}$ ), values specified in the old standard ISO 1302:1992 [18]. The input variables to be used in the study will be layer height, print speed, extruder temperature, number of perimeters and angle. Different classification algorithms will be used to solve the problem, so as to determine the one that provides the better model.

## 2 Materials and methods

The methodology used in this paper consists of several steps (Fig. 1). First, a Design Of Experiments (DOE) was developed; the DOE served as a guide during the experimental stage. Secondly, the roughness data were prepared, an essential step before data processing with the machine learning software. Thirdly, the models were generated and evaluated. Subsequently, the models were improved using ensemble

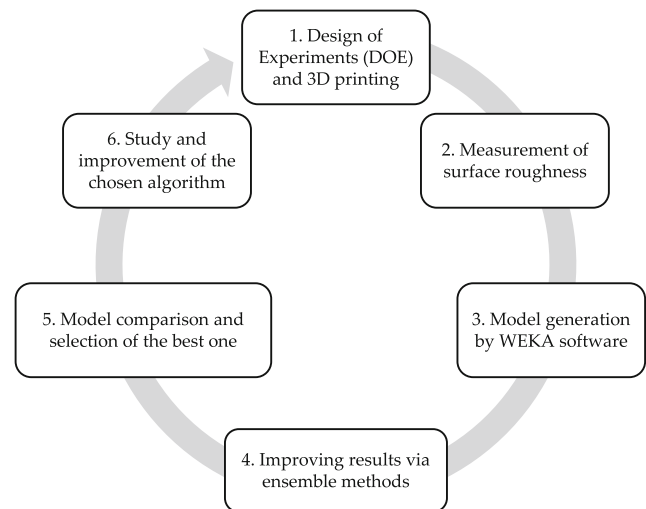


Fig. 1 Stages followed in the present work

methods. Once the model with the best results had been selected, its optimization was studied. The final stage consisted of selecting the most suitable model and presenting the results.

### 2.1 Design of Experiments (DOE) and 3D printing

In the present work, 16 specimens were printed, with a geometry shown in Fig. 2. Each of the specimens had three sloping surfaces, which formed different angles on the horizontal: 30°, 45°, and 75° (a total of 48 sloping surfaces were studied). The geometry is similar to that used by Kuo *et al.* [21] in their study of surface finish by polishing with acetone. This geometry was selected due to the absence of any international standards on surface roughness evaluation in parts printed on ABS, as previous works have outlined [16, 17].

Specimens were printed following a fractionated orthogonal experimental design (DOE) [22]. The DOE included five parameters with two or three levels per parameter. The parameters studied and the values chosen for each level are shown in



Fig. 2 Example of the geometry of the specimens used in this work. Each specimen has three surfaces: surface 1 forms a 45° angle with the horizontal; surface 2 forms a 75° angle with the horizontal; and surface 3 forms a 30° angle with the horizontal

Table 1. The values used in the manufacture of each of the surfaces under study are shown in Table 2.

The samples were produced using a Flashforge Creator Pro printer (Flashforge, ZheJiang, China). The material used for the printing was polyvinyl butyral, supplied by Smart Materials (Smart Materials, Jaen, Spain), in a 750-g roll, under the commercial name of Glace.

## 2.2 Measurement of surface roughness

Once the specimens had been printed, their surface roughness was measured on each of their sloping faces. A Mitutoyo perthometer model SJ-201 (Mitutoyo, Kawasaki, Japan) was used for this purpose. To facilitate the operation, three ABS supports were manufactured, using 3D printing (Fig. 3). Five measurements of the arithmetic average height ( $Ra$ ) were made on each of the faces. The measurements were made in the direction perpendicular to the extrusion path of the filament. A representative value was calculated from those five values using the arithmetic mean.

ISO 1302:1992 grades surface roughness based on NX classes. For example, values between 12.5 and 25  $\mu\text{m}$  are considered N11, while values between 25 and 50  $\mu\text{m}$  are considered N12. Precisely, the average values obtained in this work belong to one or the other class. Therefore, it has been decided to use the value of 25  $\mu\text{m}$  to classify these values: values under 25  $\mu\text{m}$  belong to class N11; values over 25  $\mu\text{m}$  belong to class N12.

## 2.3 Generation of model with the WEKA software

A total of 40 models were trained and validated with the measured data. The WEKA machine learning software (WEKA, University of Waikato, New Zealand) was used for this purpose. WEKA is an open-source analytical tool implemented in Java with different classification algorithms. It is used in many different application areas such as, for example, manufacturing [23–27]. WEKA offers several advantages: (1) it is freely available under the GNU General Public License; (2) it is portable since it is fully implemented in the Java programming language and thus runs on almost any architecture; and (3) it

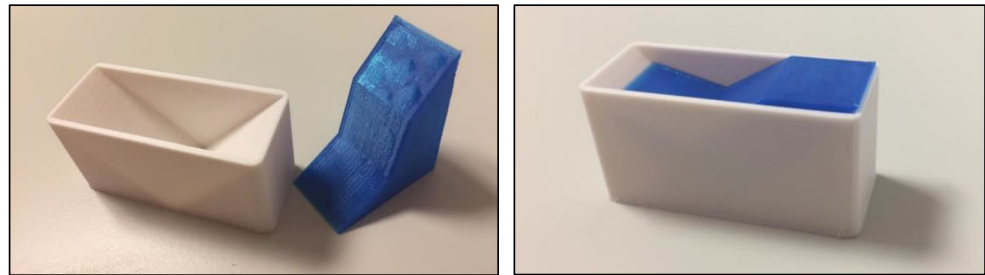
**Table 2** Values of the different parameters used for the printing of each of the surfaces studied in this work ( $LH$ , layer height;  $PS$ , print speed;  $NP$ , number of perimeters;  $T$ , extruder temperature;  $WA$ , wall angle)

Surface	LH (mm)	PS (mm/s)	NP (unit)	T (°C)	WA (°)
1	0.15	40	2	210	45
2	0.15	40	2	210	75
3	0.15	40	2	210	30
4	0.15	40	2	230	45
5	0.15	40	2	230	75
6	0.15	40	2	230	30
7	0.15	40	5	210	45
8	0.15	40	5	210	75
9	0.15	40	5	210	30
10	0.15	40	5	230	45
11	0.15	40	5	230	75
12	0.15	40	5	230	30
13	0.15	80	2	210	45
14	0.15	80	2	210	75
15	0.15	80	2	210	30
16	0.15	80	2	230	45
17	0.15	80	2	230	75
18	0.15	80	2	230	30
19	0.15	80	5	210	45
20	0.15	80	5	210	75
21	0.15	80	5	210	30
22	0.15	80	5	230	45
23	0.15	80	5	230	75
24	0.15	80	5	230	30
25	0.25	40	2	210	45
26	0.25	40	2	210	75
27	0.25	40	2	210	30
28	0.25	40	2	230	45
29	0.25	40	2	230	75
30	0.25	40	2	230	30
31	0.25	40	5	210	45
32	0.25	40	5	210	75
33	0.25	40	5	210	30
34	0.25	40	5	230	45
35	0.25	40	5	230	75
36	0.25	40	5	230	30
37	0.25	80	2	220	45
38	0.25	80	2	220	75
39	0.25	80	2	220	30
40	0.25	80	2	210	45
41	0.25	80	2	210	75
42	0.25	80	2	210	30
43	0.25	80	5	220	45
44	0.25	80	5	220	75
45	0.25	80	5	220	30
46	0.25	80	5	210	45
47	0.25	80	5	210	75
48	0.25	80	5	210	30

**Table 1** Parameters studied and values established for each level

Parameter	Level 1	Level 2	Level 3
Layer height, LH (mm)	0.15	0.25	–
Print speed, PS (mm/s)	40	80	–
Number of perimeters, NP (unit)	2	5	–
Extruder temperature, T (°C)	210	220	230
Wall angle, WA (°)	30	45	75

**Fig. 3** Example of a support manufactured to facilitate the measurement of one of the sides of the printed piece



encompasses a huge collection of data preprocessing and modeling techniques.

The machine learning process began by analyzing the input data from two indicators, the value of the correlation and the information gain:

- Correlation evaluates the value of an attribute by measuring the Pearson's correlation coefficient between the attribute and the class. Nominal attributes are considered on a value-by-value basis by treating each value as an indicator. An overall correlation for a nominal attribute is arrived at via a weighted average. It takes the value of 1 for perfect correlations and 0 for losses [28].
- Information gain is the amount of information that is gained by knowing the value of an attribute. It is related to entropy, which is the degree to which a system does not follow a particular pattern and is given by a function that satisfies the Eq. (1). Information gain is the entropy of the distribution before the split minus the entropy of the distribution after it.

$$\text{Information}_{1,2}(p_1 p_2) = \text{Information}_1(p_1) + \text{Information}_2(p_2) \quad (1)$$

where:

- $p_1 p_2$  is the probability of event 1 and event 2
- $p_1$  is the probability of event 1
- $p_2$  is the probability of event 2

The algorithms used in the present work are summarized in Table 3. These classifiers are traditionally grouped into five major categories: rules, functions, Bayes, lazy and trees. The rules algorithms are not predictive, but use certain rules to classify the data; functions are algorithms that estimate a function; Bayes algorithms are based on Bayes' Theorem; lazy algorithms use lazy learning and trees algorithms create decision trees. Finally, some ensembles techniques were also selected to analyze whether they could improve the results achieved by base classifiers. Ensemble methods are meta-algorithms, a powerful tool that combines the predictions of

various algorithms with the aim of decreasing variance, bias and improving predictions. The ensemble methods under consideration are shown in Table 4. To the best knowledge of the authors, the lengthy list of selected algorithms, compiled in Tables 3 and 4, represents the most extensive test of different machine learning algorithms for FDM modeling. Far fewer algorithms have been presented in previous studies [15]. The list includes Artificial Neural Networks that can in fact be considered a standard for the modeling of this industrial task. Although there are other types of machine learning algorithms that are not considered in this research, the extensive selection of different families might be enough to find a suitable algorithm for modeling this industrial task in terms of industrial standards.

Two different strategies were followed in the algorithm tuning process. The first was applied to the ANNs (MLPs in this research) while the second strategy was applied to the other machine learning algorithms that had been selected. In the case of MLPs, a grid search tuning for the number of neurons in the hidden layers and the number of hidden layers was followed. The default values proposed by WEKA for the parameters of the other algorithms were used. This double strategy was based on previous works that have outlined the high sensitivity of neural networks to the parameter tuning process in small datasets (in terms of instances number) compared with the other families of machine learning techniques [23].

## 2.4 Model comparison and selection of the best one

The parameters that correctly classified instances and the kappa statistics were analyzed to select the best model:

- Correctly classified instances (accuracy): this parameter measures the relationship between the correctly classified instances (true positive and true negative) against the total of instances in percentage terms. It is calculated as shown in Eq. (2).

$$\text{Accuracy} = \frac{\text{true positive} + \text{true negative}}{\text{total observations}} \times 100 \quad (2)$$

**Table 3** Description of the data mining algorithms used in the present work (elaborated from [29])

Classifier	Algorithm	Description	Ref.
Functions	Logistic	Logistic regression is a statistical model that predicts the probability of some events occurring as a linear function of a set of predictor variables. The algorithm learns a coefficient for each input value, which is linearly combined into a regression function and transformed using a logistic (s-shaped) function.	[29–35]
Functions	Multilayer perceptron (MLP)	MLP is a feed-forward neural network with one or more hidden layers that use back-propagation to classify instances. The structure of a MLP typically consists of input layer, hidden layers, and output layer, where the input signals are propagated in forward direction.	[36]
Functions	Sequential minimal optimization (SMO)	It is a support vector machine (SVM) classifier that employs sequential minimal optimization for training. SVM works by finding a line that best separates the data. This is done using an optimization process that only considers those instances, called support vectors, in the training dataset that are closest to the line that best separates the classes.	[37]
Bayes	Bayes net	It is a Bayesian classification algorithm which provides joint conditional probability distributions. BN algorithm consists of a directed acyclic graph and a set of conditional probability tables. Each random variable is expressed by a node in the directed acyclic graph. The conditional probability table for the values of the variables indicates each possible combination of the values of its parent nodes.	[37]
Bayes	Naïve-Bayes	It is a classification algorithm which is based on Bayes’ theorem. The suppositions of accepting that predictive attributes are conditionally independent given the class and no hidden or latent attributes influence the predictive process make the algorithm a suitable tool for classification and learning. It calculates the posterior probability for each class and makes a prediction for the class with the highest probability.	[38]
Lazy	IBk	It is an instance-based learning algorithm which is a slightly modified version of the K-nearest neighbor (KNN) algorithm. It works by storing the entire training dataset and querying it to locate the <i>k</i> most similar training patterns when making a prediction. The value of <i>k</i> parameter determines the size of the neighborhood. It assumes that the distance between data instances is meaningful in making predictions (the distance is calculated with functions such as Euclidean or Manhattan).	[39]
Lazy	KStar	It is an instance-based learning algorithm which uses an entropy-based distance function. It handles with symbolic attributes, real-valued attributes, and missing values properly owing to the use of entropy as a distance function. The technique of summing probabilities over all possible paths overcomes the problem of smoothness.	[40]
Trees	J48	J48 is a slightly modified version of C4.5 in WEKA. C4.5 is a successor of the ID3 algorithm. For a given set, each time the algorithm selects an attribute with the highest information gain. It works by creating a tree to evaluate an instance of data. The tree is inverted, starting at the top or root of the tree and moving down to the leaves until a prediction can be made. The process of creating a decision tree works by greedily selecting the best split point in order to make predictions and repeating the process until the tree is a fixed depth. After the tree is constructed, it is pruned in order to improve the model.	[29–41]
Trees	Logistic model trees (LMT)	LMT is a classification algorithm that integrates decision tree induction with logistic regression. The tree structure of the algorithm is grown in a similar manner to the C4.5 algorithm. Here, an iterative training of additive logistic regression models is performed. By splitting, the logistic regressions of the parent node are passed to the child nodes. This provides to have all parent models and probability estimates for each class at the leaf nodes of the final model.	[42]
Trees	Random forest	It is an ensemble of classification or regression trees, induced from bootstrap samples of the training data. In this model, the generalization error of the classifier depends on the power of the individual trees and the association between the trees. Random feature selection is used in the tree induction process. This enables algorithm to perform comparable to the Adaboost algorithm and to be tolerable with noisy data. Trees Algorithms	[43]

- Kappa statistic: this parameter measures the agreement between predicted and observed categorizations of a dataset, while correcting for agreement that occurs by chance. Values close to unity indicate higher concordance (Table 5).

Finally, once the most accurate algorithm had been selected, their performance was studied in detail. The

aim of this stage was to select the most appropriate values for the parameters of the algorithm, so that the model will have the best possible predictive capacity. The fine tuning of the most-accurate algorithm was therefore performed, to study the effect of the parameter tuning procedure on model accuracy. This tuning procedure followed a grid search as will be presented in detail in the following section.



**Table 4** Description of the data mining ensemble methods

Ensemble methods	Description	Ref.
Bagging	It consists of building a set of $n$ random samples of the data and training different algorithms on those samples. Each model creates a prediction, and the result is the average of all the models. This technique is useful when you have a limited amount of data with low bias and high variance.	[44]
Boosting	It is similar to Bagging but uses a more ingenious technique since in each iteration, it tries to correct the errors made previously by giving more weight to the data that have been misclassified. Subsequent models are trained and added until a minimum accuracy is achieved or no further improvements are possible. Each model is weighted based on its skills, and these weights are used when combining the predictions from all of the models on new data.	[30]
Random subspace	It combines multiple trained classifiers in subspaces of randomly selected entities. It aims to avoid overadjustment while providing high accuracy.	[30]

### 3 Results and discussion

#### 3.1 Average surface roughness of each printed surface

Table 6 shows the average values of surface roughness  $Ra$  ( $\mu\text{m}$ ), obtained as an arithmetic mean of the five measurements made on each surface. To analyze the data, two classes were created: the first class (N11, according to ISO 1302:1992) corresponded to those  $Ra$  values with values lower than  $25 \mu\text{m}$ ; the second class (N12, according to ISO 1302:1992) corresponded to those  $Ra$  values with a value higher than or equal to  $25 \mu\text{m}$ . In those samples where it was not possible to measure  $Ra$ , due to its high value, the surface was considered as class N12.

These experimental results are consistent with those published by other authors who have studied this same problem. Boschetto *et al.* [16] studied the relationship between wall angle and surface roughness for different materials (ABS, ABS plus, Polycarbonate, ULTEM 9085). For layer height  $0.254 \text{ mm}$ , the surface roughness was low ( $Ra < 30 \mu\text{m}$ ), between  $40^\circ$  and  $140^\circ$  (in the present work, it would coincide with the interval  $0\text{--}50^\circ$ ), while it was high ( $Ra > 30 \mu\text{m}$ ) between  $0^\circ$  and  $40^\circ$  (in the present work, it would coincide with the interval  $50\text{--}90^\circ$ ).

**Table 5** Meaning of the Kappa statistic parameter

Range	Kappa
0.00	Poor
0.01–0.20	Slight
0.21–0.40	Fair
0.41–0.60	Moderate
0.61–0.80	Substantial
0.81–1.00	Almost perfect

#### 3.2 Influence of the printing parameters on surface roughness

The problem type is ‘classification’ since the output is a nominal type of category. There are five input attributes. First, an analysis is performed to see which attribute has the most influence on the class. To do so, both the correlation and information gain are used. Correlation determines how much two attributes change together, either in the same or differing directions on the number line. The information gain calculates the information for each attribute for the output variable. Entry values vary from 0 (no information) to 1 (maximum information) [30]. Table 7 shows that wall angle (correlation = 0.6325; info gain = 0.344) and layer height (correlation = 0.5071; info gain = 0.196) are the two attributes with the highest influence on the output variable. The other factors analyzed (print speed, extruder temperature, number of perimeters) have much lower correlation and info gain values.

In flat geometry parts, models are usually generated by setting the layer height and using the wall angle as the only input variable for models generated by neural networks [16]. Vahabli and Rahmati [17] calculated the relative importance of both factors in these types of problems using Garson's algorithm. The wall angle yielded a Relative Importance (RI) of around 60% for different models, while the layer height yielded an RI of around 40%. Results that were consistent with the results of this study.

Li *et al.* [15] selected the following features as the most influential on the surface roughness of 3D printed flat parts using FDM: frequency amplitude of the build plate vibrations, the extruder vibrations, the temperature of the build plate, and the extrusion temperature. For parts with a cylindrical geometry, the layer height and the number of perimeters appear as the most influential variables [31]. However, it cannot be said that those conclusions were consistent with the results of this work.

**Table 6** Average value of surface roughness ( $Ra$ ) for each surface and class it belongs to

Specimen	$Ra$ ( $\mu\text{m}$ )	Class	Specimen	$Ra$ ( $\mu\text{m}$ )	Class	Specimen	$Ra$ ( $\mu\text{m}$ )	Class
1	23.38	N11	17	30.54	N12	33	27.75	N12
2	30.84	N12	18	18.60	N11	34	32.91	N12
3	12.70	N11	19	26.71	N12	35	38.25	N12
4	23.64	N11	20	31.71	N12	36	28.49	N12
5	29.62	N12	21	26.65	N12	37	36.59	N12
6	23.49	N11	22	21.80	N11	38	> 25.00	N12
7	22.87	N11	23	31.10	N12	39	> 25.00	N12
8	28.15	N12	24	15.28	N11	40	33.83	N12
9	18.65	N11	25	34.57	N12	41	> 25.00	N12
10	23.94	N11	26	51.69	N12	42	26.10	N12
11	29.39	N12	27	26.65	N12	43	35.32	N12
12	15.98	N11	28	33.32	N12	44	> 25.00	N12
13	22.35	N11	29	44.41	N12	45	> 25.00	N12
14	32.25	N12	30	26.65	N12	46	34.46	N12
15	19.90	N11	31	34.52	N12	47	> 25.00	N12
16	23.34	N11	32	51.37	N12	48	> 25.00	N12

The values of surface roughness that could not be measured were considered higher than 25  $\mu\text{m}$  (class N12)

### 3.3 Base classifiers performance

The main classification algorithms have been evaluated according to the type of classification they perform. Figure 4 shows the results obtained through training with the 48 instances of the most common classification algorithms. The base algorithms with the best results are SMO and Multilayer Perceptron.

Both algorithms are widely used in the literature:

- Support vector machine or SVM (programmed in WEKA as SMO). Aoyagi *et al.* [19] used a model generated via SVM to predict the class of surface roughness (good or bad) in parts produced via powder-bed fusion-type AM technology. Hu *et al.* [32] also used the SVM algorithm to determine which printing temperatures were most suitable for normal FDM printing, and to avoid warping or insufficient filling problems.
- Neural network (programmed in WEKA as Multilayer Perceptron, MLP). Neural networks are a widely used

type of algorithm in additive manufacturing, due to their strong computational power and sophisticated algorithm architecture [33]. Although they are often used to model regression problems, they are also used to solve classification problems [34].

### 3.4 Ensemble methods performance

Using ensemble methods improves the results in some combinations. Figure 5 shows the correctly classified instances for each algorithm, without using ensemble method or using one of the mentioned ensembles (Bagging, AdaBoost and Random Subspace). In this figure, it clearly appears that the best performing ensemble method is Bagging. The kappa statistic values are shown in Figure 6. The algorithms that yielded the best results in both correctly classified instances and with the kappa statistic are Bagging + Multilayer Perceptron (BMLP). These results, obtained with parts made of polyvinyl butyral, could be extrapolated to other materials, making an error of less than 10%, according to Boschetto *et al.* [16].

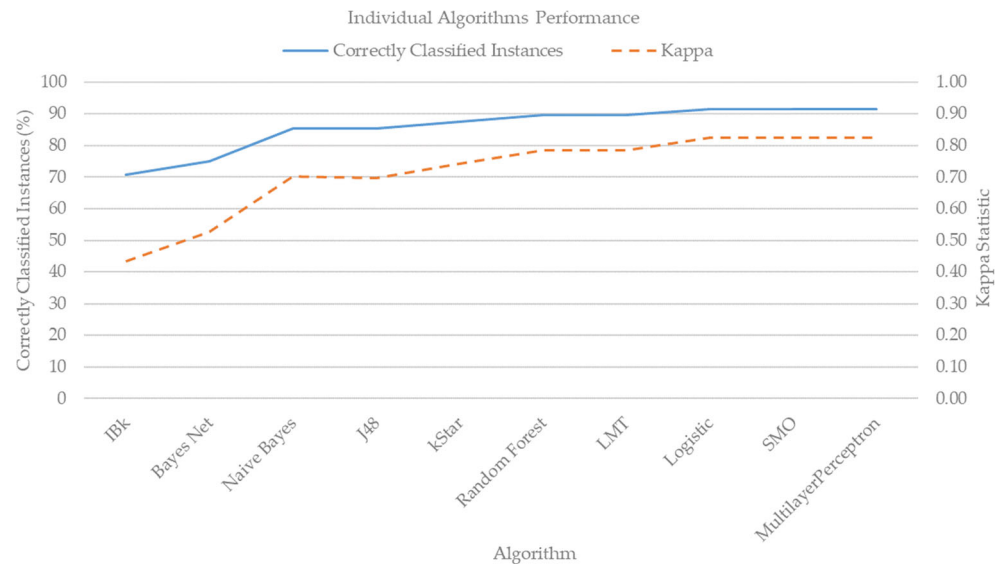
### 3.5 Tuning of the model generated by BMLP

If the neural network is appropriately configured, then the MLP algorithm can sometimes improve classification results. Therefore, in the final part of the study, work continued with the BMLP. As a default estimate, the number of neurons in the hidden layer was calculated as the mean value between the input attributes and

**Table 7** Information gain

Attribute	Correlation	Info gain
Wall angle	0.632	0.344
Layer height	0.507	0.196
Extruder temperature	0.022	0.000
Print speed	0.084	0.000
Number of perimeters	0.084	0.000

**Fig. 4** Correctly classified instances and kappa statistic obtained by the models generated by every base algorithm



the number of classes in the output variable. In this case, there were five input attributes and two classes in the output variable, so a base value of neurons in the hidden layer could be 4 neurons. These values and the number of hidden layers were modified, in order to perform the tests.

In Table 8, the number of hidden layers is represented by each level and the number of neurons in each hidden layer by the value of that level. For example, 2 means that there is one hidden layer with two neurons, 2–3 means two hidden layers, in the first hidden layer there are 2 neurons and in the second layer there are 3 neurons. As can be seen in Table 8, simple neural networks provide better results than more complex networks, because very complex models are not needed in a binary problem and the ensembles provide the stability that base models may not have.

## 4 Conclusions

In the present work, several models have been generated by means of machine learning algorithms to predict the class of surface roughness on a polyvinyl butyral printed piece printed by means of FDM. A total of ten base classification algorithms programmed in WEKA have been used for this purpose. They belong to different families of algorithms (according to WEKA: rules, functions, Bayes, lazy and trees). In addition, three ensemble methods (bagging, AdaBoost and random subspace) have been used to improve the results obtained; these ensemble algorithms are applied to the base algorithms described above: in this way, a total of 40 models have been analyzed.

The input attributes used in the study were: layer height (LH), print speed (PS), extruder temperature (T), number of perimeters (NP) and wall angle (WA). The output variable

**Fig. 5** Correctly classified instances for the different combinations of base algorithms and ensemble methods

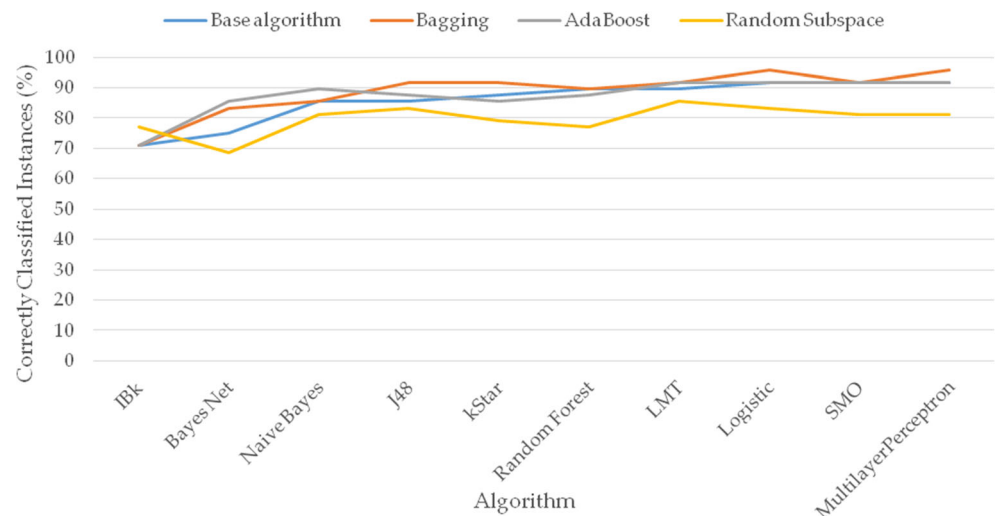
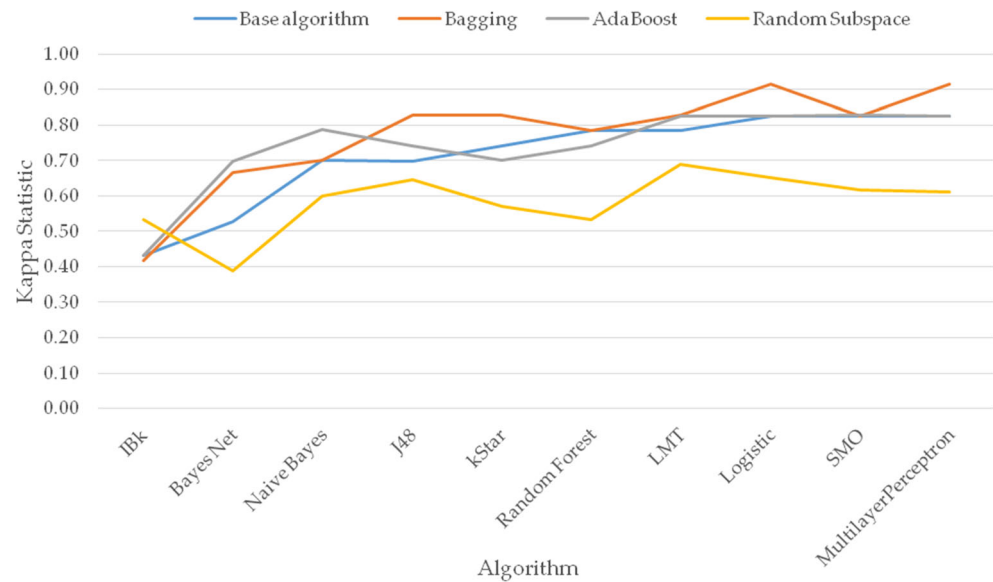




**Fig. 6** Kappa statistics for the different combinations of base algorithms and ensemble methods



was the discretized value of  $Ra$  measured on the test specimens: N11 (for surface roughness under  $25 \mu\text{m}$ ) or N12 (for values higher or equal to  $25 \mu\text{m}$ ). These values, taken from ISO 1302:1992, are often used in real workshops.

The parameters that correctly classified instances and the kappa statistic were used as the criteria to select the best model. In general, the models generated by base algorithm type functions (SMO/VSM and MLP/NN) yielded the best results. The assembly method that behaved most satisfactorily was the bagging method. Finally, the selected model has the one generated by the bagging method combined with the multilayer perceptron algorithm (BMLP). This model has been improved by using the right number of hidden layers and the right number of neurons in each layer (1 layer and 2 neurons).

One of the main qualities of polyvinyl butyral is that it becomes transparent when treated with alcohol. In future studies, we will examine the most influential variables in the

transparency of printed pieces and will try to generate models that are capable of predicting this transparency before treatment. Related to the machine learning approach, the use of multilabel classification algorithms in the near future can provide more accurate solutions for this industrial task once the other industrial outcomes such as geometrical accuracy and productivity, are considered for the experiment. Besides, the dataset will be extended to tests with FDM using other materials, to evaluate whether the information on polyvinyl butyral FDM 3D printing processes can reduce the required dataset size for new materials, thereby reducing the experimental costs. Finally, another strategy that is aimed at reducing experimental costs will be considered: the use of deep-learning algorithms for the evaluation of geometry and surface quality of FDM parts.

**Table 8** Results obtained by the BMLP algorithm for different numbers of hidden layers and different numbers of neurons per layer

Neurons-hidden layers	Correctly classified instances	Kappa statistic
2	95.833	0.914
3	95.833	0.914
4	95.833	0.914
5	95.833	0.914
6	95.833	0.914
2–2	95.833	0.914
2–3	93.750	0.870
3–2	91.666	0.826
2–2–2	60.416	0.057
3–2–3	93.750	0.870

**Author contribution** Conceptualization: [Azahara Cerro]; methodology: [Azahara Cerro and Okan Yiğit]; formal analysis: [Pablo E. Romero]; funding acquisition: [Pablo E. Romero and Andres Bustillo]; investigation: [Azahara Cerro]; resources: [Azahara Cerro and Okan Yiğit]; validation: [Azahara Cerro and Okan Yiğit]; supervision: [Pablo E. Romero and Andres Bustillo]; writing and original draft: [Azahara Cerro and Okan Yiğit]; writing, review and editing: [Pablo E. Romero and Andres Bustillo]. All authors have read and agreed to the submitted version of the manuscript.

**Funding** This work was partially supported by the SMART-EASY project (Reference Number IDI-20191008) funded by the Spanish Centro para el Desarrollo Tecnológico e Industrial (CDTI) and by the Plan Propio de Investigación of the University of Cordoba.

**Availability of data and material** Experimental data is included in Table 6.

**Code availability** All software code is included in Weka release 3.8.

## Declarations

**Competing interests** The authors declare that they have no competing interests.

## References

- Wang C, Tan XP, Tor SB, Lim CS (2020) Machine learning in additive manufacturing: state-of-the-art and perspectives. *Addit Manuf* 36:101538. <https://doi.org/10.1016/j.addma.2020.101538>
- Razvi S, Feng S, Narayana A, et al (2019) A review of machine learning applications in additive manufacturing. In: *Proceedings of the ASME 2019 international design engineering technical conferences and computers and information in engineering conference*. Anaheim (CA, USA), pp 1–10
- Meng L, McWilliams B, Jarosinski W, Park HY, Jung YG, Lee J, Zhang J (2020) Machine learning in additive manufacturing: a review. *Jom* 72:2363–2377. <https://doi.org/10.1007/s11837-020-04155-y>
- Ngo TD, Kashani A, Imbalzano G, Nguyen KTQ, Hui D (2018) Additive manufacturing (3D printing): a review of materials, methods, applications and challenges. *Compos Part B Eng* 143:172–196. <https://doi.org/10.1016/j.compositesb.2018.02.012>
- Moreno R, Carou D, Carazo-Álvarez D, Gupta MK (2020) Statistical models for the mechanical properties of 3D printed external medical aids. *Rapid Prototyp J* 27:176–186. <https://doi.org/10.1108/RPJ-02-2020-0033>
- Mangat AS, Singh S, Gupta M, Sharma R (2018) Experimental investigations on natural fiber embedded additive manufacturing-based biodegradable structures for biomedical applications. *Rapid Prototyp J* 24:1221–1234. <https://doi.org/10.1108/RPJ-08-2017-0162>
- Singh S, Singh N, Gupta M, Prakash C, Singh R (2019) Mechanical feasibility of ABS/HIPS-based multi-material structures primed by low-cost polymer printer. *Rapid Prototyp J* 25:152–161. <https://doi.org/10.1108/RPJ-01-2018-0028>
- Raju M, Gupta MK, Bhanot N, Sharma VS (2019) A hybrid PSO–BFO evolutionary algorithm for optimization of fused deposition modelling process parameters. *J Intell Manuf* 30:2743–2758. <https://doi.org/10.1007/s10845-018-1420-0>
- Mohamed OA, Masood SH, Bhowmik JL (2015) Optimization of fused deposition modeling process parameters : a review of current research and future prospects. *Adv Manuf* 3:42–53. <https://doi.org/10.1007/s40436-014-0097-7>
- Jiang J, Hu G, Li X, Xu X, Zheng P, Stringer J (2019) Analysis and prediction of printable bridge length in fused deposition modelling based on back propagation neural network. *Virtual Phys Prototyp* 14:253–266. <https://doi.org/10.1080/17452759.2019.1576010>
- Mohamed OA, Masood SH, Bhowmik JL (2016) Investigation of dynamic elastic deformation of parts processed by fused deposition modeling additive manufacturing. *Adv Prod Eng Manag* 11:227–238. <https://doi.org/10.14743/apem2016.3.223>
- Bayraktar Ö, Uzun G, Çakiroğlu R, Guldaz A (2017) Experimental study on the 3D-printed plastic parts and predicting the mechanical properties using artificial neural networks. *Polym Adv Technol* 28:1044–1051. <https://doi.org/10.1002/pat.3960>
- Sood AK, Equbal A, Toppo V, Ohdar RK, Mahapatra SS (2012) An investigation on sliding wear of FDM built parts. *CIRP J Manuf Sci Technol* 5:48–54. <https://doi.org/10.1016/j.cirpj.2011.08.003>
- Sood AK, Ohdar RK, Mahapatra SS (2012) Experimental investigation and empirical modelling of FDM process for compressive strength improvement. *J Adv Res* 3:81–90. <https://doi.org/10.1016/j.jare.2011.05.001>
- Li Z, Zhang Z, Shi J, Wu D (2019) Prediction of surface roughness in extrusion-based additive manufacturing with machine learning. *Robot Comput Integr Manuf* 57:488–495. <https://doi.org/10.1016/j.rcim.2019.01.004>
- Boschetto A, Giordano V, Veniali F (2013) Surface roughness prediction in fused deposition modelling by neural networks. *Int J Adv Manuf Technol* 67:2727–2742. <https://doi.org/10.1007/s00170-012-4687-x>
- Vahabli E, Rahmati S (2017) Improvement of FDM parts' surface quality using optimized neural networks—medical case studies. *Rapid Prototyp J* 23:825–842. <https://doi.org/10.1108/RPJ-06-2015-0075>
- ISO 1302 (1992) Technical drawings—method of indicating surface texture, International Organization for Standardization (ISO), Geneva, Switzerland
- Aoyagi K, Wang H, Sudo H, Chiba A (2019) Simple method to construct process maps for additive manufacturing using a support vector machine. *Addit Manuf* 27:353–362. <https://doi.org/10.1016/j.addma.2019.03.013>
- 3d SM (2021) Smart Materials 3D. <https://www.smartmaterials3d.com/en/>. Accessed 5 Jan 2021
- Kuo CC, Chen CM, Chang SX (2017) Polishing mechanism for ABS parts fabricated by additive manufacturing. *Int J Adv Manuf Technol* 91:1473–1479. <https://doi.org/10.1007/s00170-016-9845-0>
- Montgomery D (2020) Design and analysis of experiments, 10th edn. Wiley, Hoboken
- Munirathinam S, Ramadoss B (2016) Predictive models for equipment fault detection in the semiconductor manufacturing process. *Int J Eng Technol* 8:273–285. <https://doi.org/10.7763/ijet.2016.v8.898>
- Kittidecha C, Yamada K (2018) Application of Kansei engineering and data mining in the Thai ceramic manufacturing. *J Ind Eng Int* 14:757–766. <https://doi.org/10.1007/s40092-018-0253-y>
- Kerdprasop K, Kerdprasop N (2011) Feature selection and boosting techniques to improve fault detection accuracy in the semiconductor manufacturing process. *IMECS 2011 - Int MultiConference Eng Comput Sci 2011* 1:398–403
- Correa M, Bielza C, Pamies-Teixeira J (2009) Comparison of Bayesian networks and artificial neural networks for quality detection in a machining process. *Expert Syst Appl* 36:7270–7279. <https://doi.org/10.1016/j.eswa.2008.09.024>
- Barrios JM, Romero PE (2019) Decision tree methods for predicting surface roughness in fused deposition modeling parts. *Materials (Basel)* 12. <https://doi.org/10.3390/ma12162574>
- Ratner B (2017) Statistical and machine-learning data mining, 3rd edn. CRC Press (Taylor & Francis Group), Boca Raton
- Onan A (2015) On the performance of ensemble learning for automated diagnosis of breast cancer. Springer, Cham
- Brownlee J (2021) Machine learning mastery with Weka. Ebook. Edition: v. 1.5
- Pérez M, Medina-Sánchez G, García-Collado A, Gupta M, Carou D (2018) Surface quality enhancement of fused deposition modeling (FDM) printed samples based on the selection of critical printing parameters. *Materials (Basel)* 11(8):1–13. <https://doi.org/10.3390/ma11081382>
- Hu H, He K, Zhong T, Hong Y (2019) Fault diagnosis of FDM process based on support vector machine (SVM). *Rapid Prototyp J* 26:330–348. <https://doi.org/10.1108/RPJ-05-2019-0121>
- Qi X, Chen G, Li Y, Cheng X, Li C (2019) Applying neural-network-based machine learning to additive manufacturing: current applications, challenges, and future perspectives. *Engineering* 5:721–729. <https://doi.org/10.1016/j.eng.2019.04.012>
- Elhoone H, Zhang T, Anwar M, Desai S (2020) Cyber-based design for additive manufacturing using artificial neural networks for

- Industry 4.0. *Int J Prod Res* 58:2841–2861. <https://doi.org/10.1080/00207543.2019.1671627>
35. Witten IH, Frank E, Hall MA (2016) *Data mining: practical machine learning tools and techniques*, 4th edn. Morgan Kaufmann, Burlington
  36. Negnevitsky M (2005) *Artificial intelligence: a guide to intelligent systems*. Addison-Wesley, Reading
  37. Han J, Kamber M, Pei J (2011) *Data mining: concepts and techniques*. Morgan Kaufmann Publishers, Inc., San Francisco
  38. John G, Langley P (1995) Estimating continuous distributions in Bayesian classifiers. In: *Proc. of the eleventh conference on uncertainty in artificial intelligence*. Morgan Kaufmann Publishers, Inc., San Francisco, pp 338–345
  39. Aha DW, Kibler D, Albert M (1991) Instance-based learning algorithms. *Mach Learn* 6:37–66
  40. Clearly JG, Trigg LE (1995) An instance-based learner using and entropic distance measure. In: *Proc. Twelfth International Conference on Machine Learning*. Morgan Kaufmann Publishers, Inc., San Francisco, pp 108–114
  41. Quinlan JR (2014) *C4.5: programs for machine learning*. Morgan Kaufmann Publishers, Inc., San Mateo
  42. Landwehr N, Hall M, Frank E (2005) Logistic model trees. *Mach Learn* 59:161–205
  43. Breiman L (2001) Random forest. *Mach Learn* 45:5–32. <https://doi.org/10.1023/A:1010933404324>
  44. Breiman L (1996) Bagging predictors. *Mach Learn* 24:123–140

**Publisher's note** Springer Nature remains neutral with regard to jurisdictional claims in published maps and institutional affiliations.